Universität Hamburg

Synchrotron Research Institute

YEREVAN STATE UNIVERSITY

German-Armenian Joint Practical Course
on Accelerator Physics

Generation and Acceleration of Ultrashort Electron Beams

Supervisor: Dr. Bagrat Grigoryan

Federal Foreign Office

Supported by the German Federal Foreign Office under Kapitel 0504, Titel 68713

YEREVAN, ARMENIA
2019

Contents

The scope of the work:

In this work the students are supposed to gain basic knowledge on the electron emission, beam formation and acceleration processes in electron sources. The photoemission and beam acceleration processes will be presented in general details. Physical values relevant for the photoemission like the work function of the cathode material and the critical frequency of the illuminating light will be discussed as well as the dependence of the acceleration on the RF field amplitude and the RF phase. The detailed overview of the photocathode RF electron gun at the AREAL facility and the UV laser will be presented. In the experimental part of this work the dependence of extracted beam charge and energy on the RF phase will be measured and the quantum efficiency (QE) of a copper photocathode will be determined.

1. Introduction

Electron sources are key elements in numerous scientific and technical instruments as for example X-ray tubes, klystrons, electron microscopes, electron welding machines and all electron accelerators which accelerate the electrons generated in a source up to higher energies. Electron accelerators are powerful tools in fundamental research for example in colliding beam machines as the Super KEKB factory currently in operation in Japan or the former Large Electron Positron collider LEP at CERN, but they are also workhorses in applied science as in synchrotron radiation facilities, e.g. PETRA III, and Free Electron Lasers (FEL) as the European XFEL and FLASH. Many more electron accelerators are in operation for example in food irradiation facilities, for the sterilization of medical equipment and as part of cancer treatment in hospitals. Today an estimated number of about 30.000 accelerators are in operation worldwide. The majority of these accelerators are electron accelerators.

The performance of electron accelerators depends in general directly on the performance of the electron source because the quality of the electron beam is determined at the source. Possibilities to improve the quality during the acceleration process are limited.

On a basic level sources delivering a constant flow of particles, i.e. a DC current are distinguished from sources delivering particles in form of bunches. While a quality figure of DC beams is the current, the charge and the bunch length are figures of merit for bunched beams. Another figure of merit is the so-called transverse beam emittance which is a measure for the divergence of a beam. A small emittance allows to focus the beam to very small beam sizes and also to transport it over a longer distance without the necessity to refocus it.

The focus of this experiment is the emission process and the initial part of the acceleration from the cathode up to about 3 MeV beam energy. The transverse emittance will not be discussed, it is the worked out in experiment [1]. Thus we will concentrate on the beam charge, the gain of energy and the formation of a bunch in the gun.

The design of electron sources differs fundamentally by the basic emission process, which is employed and by the acceleration technology chosen by the designer. In the following the main emission processes will be discussed followed by a presentation of space charge limits of the emission as they occur in the main acceleration configurations, i.e. the acceleration of a DC current in a diode configuration and the emission of short electron bunches as it is typical for the acceleration in an RF field.

2. The emission process

2.1 Thermal emission

Electrons cannot leave a metal at room temperature because their energy is too low to overcome the potential barrier defined by the work function of the material. When the temperature of the material is increased some electrons gain enough energy to escape from the metal. They form a cloud of electrons (Figure 1), which can be extracted by applying an extraction voltage.

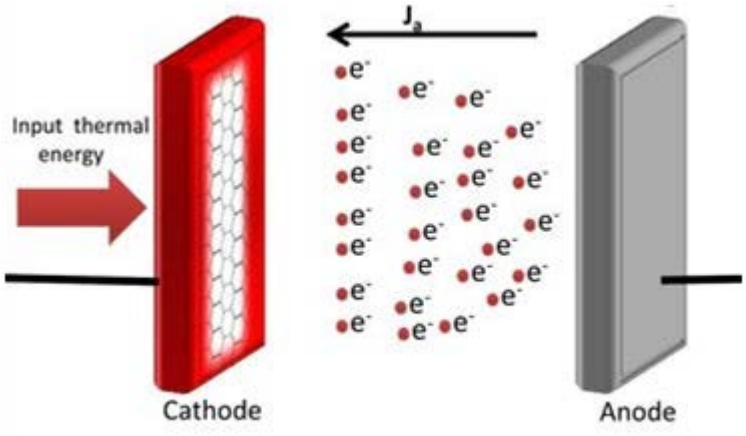

Figure 1. Thermal emission model

Thermal emission is described by the Richardson equation, which relates the current density *j* with the temperature of the material *T* as:

$$j = AT^2 \exp\left(-\frac{e\phi_e}{k_B T}\right) \qquad (2.1.1)$$

with the electrostatic potential of the material ϕ_e, the Boltzmann constant k_B, and the Richardson constant $A = \frac{4\pi mek_B^2}{h^3}$ ~ *1.202×10*^{6} *A m*$^{-2}$ *K*$^{-2}$, where *m* is the mass of an electron, *e* is elementary charge, and *h* is Planck's constant.

In practice a (material dependent) correction factor of the order of 0.5 has to be applied to *A*.

The product of electrostatic potential with elementary charge is called work function $W = e\varphi_e$. In general the work function is measured in *eV*; it has, thus, the same numerical value as the electrostatic potential.

Because of the exponential function, the current increases rapidly with temperature as long as $k_B T$ is lower than the electrostatic potential. Essentially all materials melt before $k_B T = e\phi_e$ is reached.

Thermal cathodes need to operate at high temperatures of about 1000°. Typical cathode materials are metals like Tungsten or Tantalum and compounds like CeB_6 or LaB_6. In order to reduce the electro static potential and operate at lower temperatures metal cathodes can be doped for example with Thorium or Barium oxide.

Thermal cathodes are simple and robust and most suitable for applications which require a DC current. The DC current of a thermal cathode can be modulated e.g. by grids which are placed in the beam path. The minimal pulse length is however limited to the nanosecond range. A disadvantage of thermionic cathodes is the limited current density of not more than about ~10^5 A/m^2.

2.2 Field emission

Field emission is based on the quantum mechanical tunnel effect. Figure 2 shows schematically the potential near the surface of a metal with a step-like electrostatic potential. When a strong external field is applied the potential barrier bends down and electrons can tunnel through the barrier.

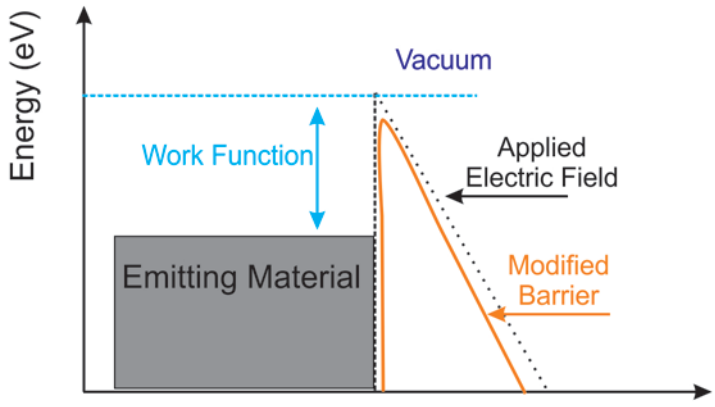

Figure 2. Potential near the emitter surface

The process requires very high field gradients of the order of 1 GeV/m and thus one might expect that it is not relevant for practical applications. However, very near to the surface of any high voltage device the field can be enhanced by irregularities like scratches, sharp edges or microscopic dust particles. In the field emission theory this field enhancement is taken into account by the field enhancement factor β and an effective emitting area A_e. Field emission follows the Fowler-Nordheim equation [2]:

$$I_F = \frac{5.7\times10^{-12}\times10^{4.52W^{-0.5}}A_e(\beta E_0)^{2.5}}{W^{1.75}} \times \exp\left[\frac{-6.53\times10^{9}\times W^{1.5}}{\beta E_0}\right], \quad (2.2.1)$$

where *W*- is the work function measured in *eV* and E_0 - is the externally applied field.

In this form Eq.(2.2.1) is applicable for RF fields, i.e. the temporal variation of the field is already taken into account and I_F - is the average current over an RF cycle.

In order to make use of field emission as electron source tungsten filaments are etched down to very sharp needles. These filaments are used for example in high performance electron microscopes. The current density which can be drawn from field emission cathodes is extremely high (10^{10}-10^{11} A/m^2) the total current is however very small (~ pA), because the effective cathode area is on the order of square nanometers, see Figure 3 for an example.

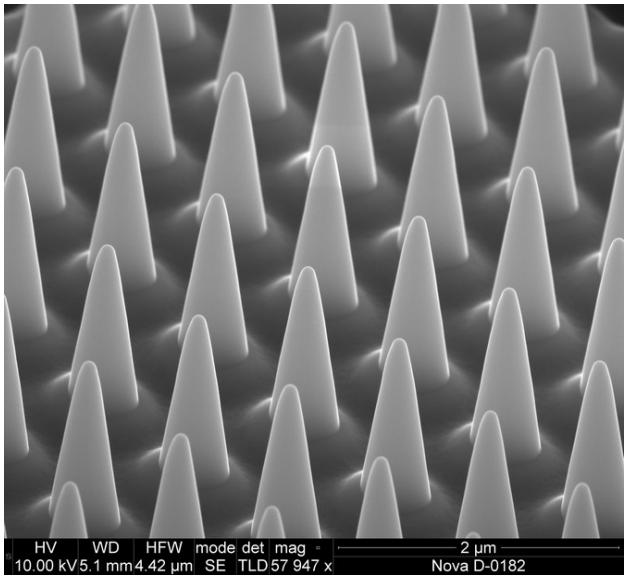

Figure 3. Array of field emitting tips.

Since electrons can be field emitted from all imperfections on the surface of high voltage devices the process of field emission is relevant in all electron sources. Note the exponential dependence of the field emission on the applied gradient. Field emission is the basic mechanism which leads to break downs when the voltage is increased. The surface of high voltage devices needs hence to be as smooth and as clean as possible. Even when the surface is prepared with great care, electrons will be field emitted in an uncontrolled way in all high voltage devices. A part of these electrons will be accelerated together with the intentionally produced beam and will

form an undesired background which is called dark current. Dark current can severely limit the performance of electron sources and accelerating cavities. The generation of dark current [3] and the means to suppress the emission dark current (e. g. polishing and cleaning) are subject of intense studies.

2.3 Photoemission

The release of electrons from a material (metal or semiconductor) through excitation by photons is called photoemission (Figure 4).

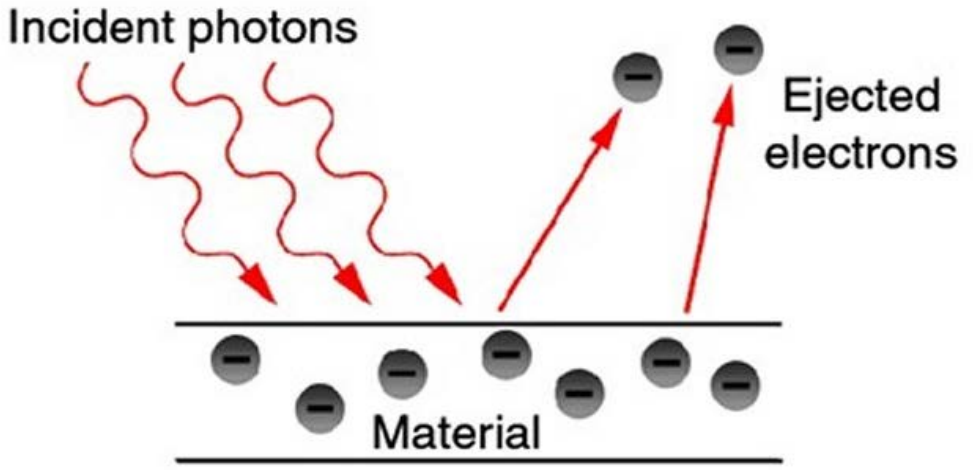

Figure 4: Illustration of the photoemission process.

In 1905 Einstein explained the photoelectric effect by applying Planck's hypothesis of energy quantization. The photoelectric effect describes the emission of electrons from a metal surface, which is irradiated by light, typically in the UV frequency range. It was observed, that the kinetic energy of the emitted electrons depends on the frequency ν of the radiation and that any material is characterized by a threshold frequency ν_o, below which no electrons are emitted. The intensity of the incident light influences the number of emitted electrons, but not the kinetic energy of the electrons. Einstein showed that these results can be explained by two assumptions:

- the energy of light is quantized, i.e. light has a particle character and the energy of the particle, named photon, is given by the frequency of the light multiplied by Planck's constant.
- an atom in the metal can absorb either a whole photon or nothing.

Electrons which gain energy by absorption of a photon can freely move in a metal or in the conduction band of a semiconductor. When hitting the surface a part of the kinetic energy is required to overcome the potential barrier or work function $W = e\phi_e$, the excess energy is the kinetic energy of the free electrons $E_{kin} = h\nu - e\phi$.

The work function of a uniform surface is defined as the minimum energy, required to extract an electron from a solid to a point in the vacuum far away from the solid. It is thus the difference between the electrostatic potential times the elementary charge in the vacuum nearby the solid and the Fermi level, i.e. the highest occupied energy level at zero Kelvin temperature, inside the material (Figure 5). Table 1 summarizes the work function of a number of metals.

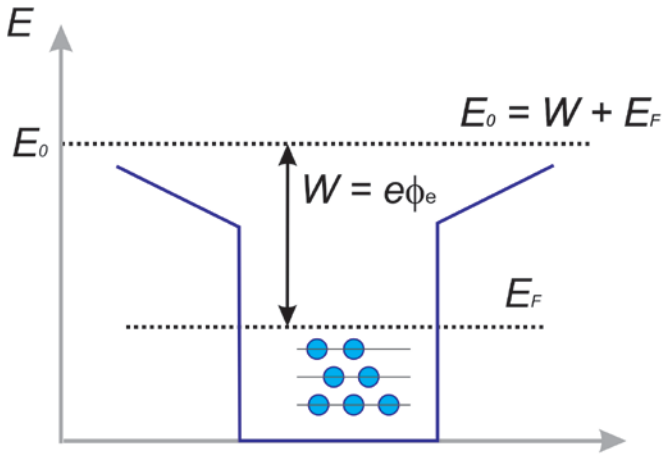

Figure 5: The potential barrier binding the electrons inside a material.

Table 1: Work function of various metals.

Metal	Work function (eV)	Metal	Work function (eV)
Al (Aluminum)	4.3	Mo (Molybdenum)	4.6
Ti (Titanium)	4.33	Ru (Ruthenium)	4.7
V (Vanadium)	4.3	Rh (Rhodium)	4.98
Cr (Chromium)	4.5	Hf (Hafnium)	3.9
Mn (Manganese)	4.1	Ta (Tantalum)	4.25
Fe (Iron)	4.7	W (Tungsten)	4.55
Co (Cobalt)	5	Re (Rhenium)	4.96
Ni (Nickel)	5.15	Os (Osmium)	4.83
Nb (Niobium)	4.3	Ir (Iridium)	5.27
Cu (Copper)	4.65	Au (Gold)	5.1

Not all excited electrons reach the surface of the cathode and overcome the potential barrier. Some travel deeper into the bulk material, some hit the surface under a shallow angle and are reflected backward because the momentum in direction perpendicular to the surface is too small, and some electrons loose energy due to scattering processes. The ratio of the number of incident photons to the number of extracted electrons is called quantum efficiency:

$$Q_E = \frac{N_e}{N_{ph}} \qquad (2.3.1)$$

The number of photons in a pulse times the energy of a photon yields the total energy of the photon pulse

$$E_{pulse} = N_{ph} h\nu \qquad (2.3.2)$$

The quantum efficiency of a material depends on various parameters as the absorption depth of the photons and energy loss mechanisms but also on the work function and thus on the details of the surface. Adsorbents on the cathode surface can, for example, lower or raise the quantum efficiency.

Due to its dependence on the details of the cathode surface and in order to understand and monitor possible cathode damage the quantum efficiency should be regularly measured.

The utilization of the photo emission process in electron sources requires a high technical effort since a short pulse laser needs to be installed and operated. Moreover require some semiconductor cathodes a special cathode system for the in-vacuum production and exchange. However, the application of the photo cathode laser enables a precise control of the emission process which improves the quality of the electron pulse significantly. Besides pulse length and transverse size of the emission spot on the cathode also the distribution (e.g. Gaussian vs. flat-top) can be optimized. Very high current densities of up to 10^7 A/m^2 can be realized which allows the production of high quality electron pulses with several nC total charge.

2.4 Schottky effect

The Schottky effect [4] describes an effective lowering of the electrostatic potential of a cathode by an externally applied field.

When an electron is moved away from the cathode surface a work has to be performed against the electrostatic force given by the charge and its mirror charge in the conducting cathode. The force reads as:

$$F(x) = -\frac{e^2}{4\pi\varepsilon_0(2x)^2} \qquad (2.4.1)$$

where *x* is the distance of the electron from the cathode surface and ε_0 is the dielectricity constant. The mirror charge has the same distance to the cathode as the electron the total distance is thus *2x*.

The potential energy of an electron at position *x* is defined by the integral:

$$E_{pot} = -\int_{\infty}^{x} F(x)dx = -\frac{e^2}{16\pi\varepsilon_0}\frac{1}{x} \qquad (2.4.2)$$

The potential energy is zero when the electron is far away from solid and it gets negative when the electron moves towards the solid.

When an external field of strength *E* is applied a linear potential needs to be added

$$E_{pot} = -\frac{e^2}{16\pi\varepsilon_0}\frac{1}{x} - eEx \qquad (2.4.3)$$

This function (Eq. 2.4.3) reaches a maximum at a distance

$$x_{max} = \sqrt{\frac{e}{16\pi\varepsilon_0 E}} \qquad (2.4.4)$$

and the value at this distance follows as

$$\Delta W = \sqrt{\frac{e^3 E}{4\pi\varepsilon_0}} \qquad (2.4.5)$$

or for the corresponding electro static potential

$$\Delta\phi = \sqrt{\frac{eE}{4\pi\varepsilon_0}} \qquad (2.4.6)$$

The lowering of the electrostatic potential leads to an increase of the quantum efficiency of a cathode. The reduction of the potential due to Schottky effect is illustrated in Figure 6.

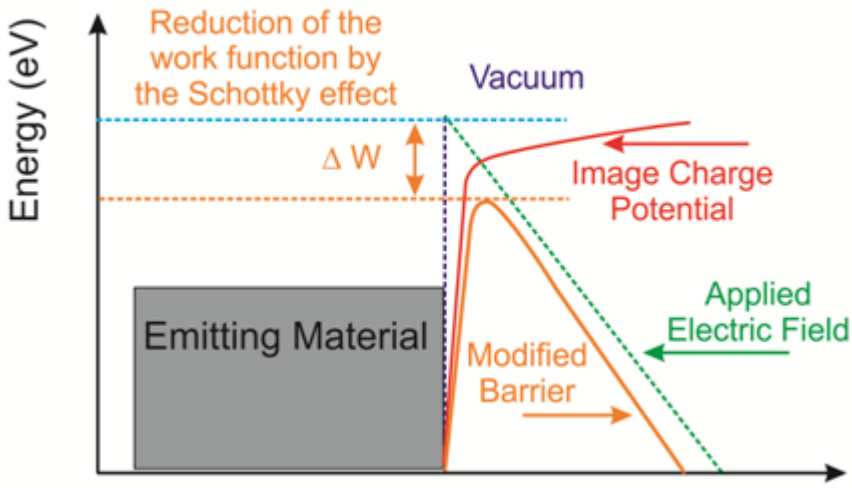

Figure 6. Reduction of electrostatic potential due to Schottky effect

3 Space charge limits in the emission process

In order to draw a current from a cathode it is necessary to apply an extraction field E_{extr} , so that electrons are accelerated away from the cathode. However, when the emission is strong the electrons cannot be removed fast enough and the electrons form a charge cloud in front of the cathode. A strong space charge field E_{spch} builds up which tends to compensate the extraction field at the cathode. When the space charge field is compensating the extraction field $E_{extr} = E_{spch}$ the so-called space charge limited emission is reached. Technically two configurations have to be distinguished: A diode configuration which is often used to generate a DC current and an RF gun which is preferably used to generate short electron bunches.

3.1 Space charge limit in a diode: The Child-Langmuir law

A diode configuration consists of a cathode – anode assembly separated by a distance *d* to which a voltage *V* is applied. The extraction field is thus $E_{extr} = V / d$. Electrons starting at the cathode leave the diode through a hole in the anode and don't contribute anymore to the space charge field at the cathode.

Considering the case of two parallel, infinite plates on a potential difference V and a uniform current density *j* pointing from one plate to the other, i.e. a transversely infinite diode gap, we can set up the following three equations to find the stationary solution of the current flow:

$$\frac{d^2\varphi}{dz^2} = -\frac{dE_z}{dz} = -\frac{\rho}{\varepsilon_0} \qquad (3.1.1)$$

$$j = \rho \cdot \dot{z} \qquad (3.1.2)$$

$$\frac{m}{2}\dot{z}^2 = e\varphi(z) \qquad (3.1.3)$$

φ - denotes the potential, m – is the rest mass of the electron, E_z is the electric field in direction of the current flow z, and ρ denotes the charge density. A dot indicates the derivation with respect to the time.

We replace the charge density ρ in Poisson's equation (Eq. 3.1.1) by $j/\dot{z}$ (from Eq. 3.1.2) and redefine the current density to become a positive quantity. The equation of energy conservation (Eq. 3.1.3) relates the particle velocity to the potential φ as:

$$\dot{z} = (2e\varphi(z)/m)^{1/2} \qquad (3.1.4)$$

which we use to replace the particle velocity in the already modified Poisson equation, which brings us to:

$$\frac{d^2\varphi}{dz^2} = \frac{j}{\varepsilon_0}\left(\frac{m}{2e}\cdot\frac{1}{\varphi}\right)^{1/2} \qquad (3.1.5)$$

Eq. 3.1.5 can be integrated after multiplication with $d\varphi/dz$ to yield:

$$\left(\frac{d\varphi}{dz}\right)^2 = \frac{4j}{\varepsilon_0}\left(\frac{m}{2e}\varphi\right)^{1/2} + C \qquad (3.1.6)$$

When the emission is space charge limited, the field on the cathode, which we locate at $z = 0$, is zero, i.e. $d\varphi/dz = 0$. Also $\varphi = 0$ at $z = 0$ and hence $C = 0$. The differential equation (3.1.6) can now be integrated to yield:

$$\varphi(z) = \left(\frac{9}{4}\frac{j}{\varepsilon_0}\right)^{2/3}\cdot\left(\frac{m}{2e}\right)^{1/3} z^{4/3} \qquad (3.1.7)$$

Denoting the distance of the plates with d so that $\varphi(d) = V$ we can resolve Eq. 3.1.7 for the space charge limited current density given as:

$$j = \frac{4}{9}\varepsilon_0\left(\frac{2e}{m}\right)^{1/2}\frac{V^{3/2}}{d^2} \qquad (3.1.8)$$

which is called Child's law or Child-Langmuir law.

3.2 Pulsed emission: The plate capacitor model

The Child-Langmuir law describes a steady state solution. Since electrons leave the diode gap at the anode side while new electrons enter the gap at the cathode the total charge contained in the gap is constant and a constant current is drawn from the cathode.

Pulse emission is fundamentally non-stationary. The first electrons are emitted into a space charge free region. While the emission continues the space charge field builds up. Usual operation parameters, i.e. pulse length and pulse energy of the photo emitting laser pulse, are chosen such that the emission is reaching the space charge limit toward the end of the photon pulse. Thus it is of fundamental importance that the emission process can be fully controlled, which is the case for photo emission but not for thermal or field emission.

Even though a high extraction field is applied in an RF gun the electrons pile up in front of the cathode due to the short emission time.

It is instructive to estimate the length of the electron pulse in front of the cathode at the end of the emission time which is given by the temporal length of the laser pulse *t* in a classical approximation.

Ignoring space charge forces and assuming particles starting with zero velocity at the cathode the position of a particle, which has been accelerated for a time *t* is given as:

$$z = \frac{e}{2m} E_\phi t^2 \qquad (3.2.1)$$

E_ϕ - is the gradient at the emission phase. For the oscillating field in an RF gun we define the phase as a sine function, i.e. at $\phi = 0$ the field changes its sign and $E_\phi = E_0 \sin(\phi)$.

We can use Eq. 3.2.1 to roughly estimate the bunch length at the end of the emission process of a short bunch. Table 2 lists the bunch length and the maximum kinetic energy, i.e. the kinetic energy in the head of the bunch for typical operation parameters of the AREAL gun.

Table 2.Bunch length and maximum kinetic energy at the end of the emission process for typical RF gun parameters. At 30 keV the particles travel with ~ 30% of the speed of light.

RF band	accel. gradient E_ϕ	emission time *t*	bunch length *z*	kinetic energy E_{kin}
S-band	64.2 MV/m	9.2 ps	~0.5 mm	~ 32 keV

Despite the high gradient the electrons form a flat cloud in front of the cathode. Since the cathode is conducting mirror charges are induced in the conducting cathode thus a double layer of charges is formed and the field on the cathode can simply be described by a plate-capacitor model as:

$$E_{spch}(t) = \frac{q(t)}{\varepsilon_0 A} \qquad (3.2.2)$$

While the Child-Langmuir law leads to a current limit, the plate-capacitor model leads to a charge limit. Not however, that even though a constant current is drawn from the diode setup the total charge contained in the diode gap is constant and only the integrated charge in the gap determines the space charge limit. Thus, also the diode is limited by an integrated charge.

4. Electron acceleration: From rest to relativistic energies

In the previous sections the emission process and the space charge limit at the cathode have been discussed. Next we need to understand in detail how the electrons are accelerated from rest to relativistic energies in a so-called RF gun (RF = Radio Frequency). An RF gun is a short radiofrequency cavity which is terminated on one side by the cathode plane, see Figure 7. A cavity is a hollow body, typically made from high conducting copper. An RF wave of wavelength λ is coupled into the cavity through the RF coupler. The dimensions of the cells are chosen such that the cells resonate with the frequency of the driving RF wave. The AREAL gun operates in the so-called S-band frequency range; the wavelength of the RF wave is 10 cm, the frequency is 2.998 GHz.

The longitudinal electric field component can reach in an RF gun a maximum at the cathode, so that electrons are very efficiently drawn away from the cathode. This is achieved by a cell length which corresponds to a quarter of a wavelength. This half-cell is followed by a full cell (half of a wavelength) in order to increase the energy further. As illustrated in the lower part of Figure 7 the oscillating field and the motion of the electrons are matched, so that the field changes it sign when the electrons leave the half-cell and enter the full cell. In this way the electron see always an accelerating field. This image is however idealized. In practice the low energy electrons shift in phase and in dependence on the starting phase may reach an accelerating or a decelerating phase in the full cell. The dynamics of the acceleration process is thus the topic of the following discussion, which follows closely reference [5].

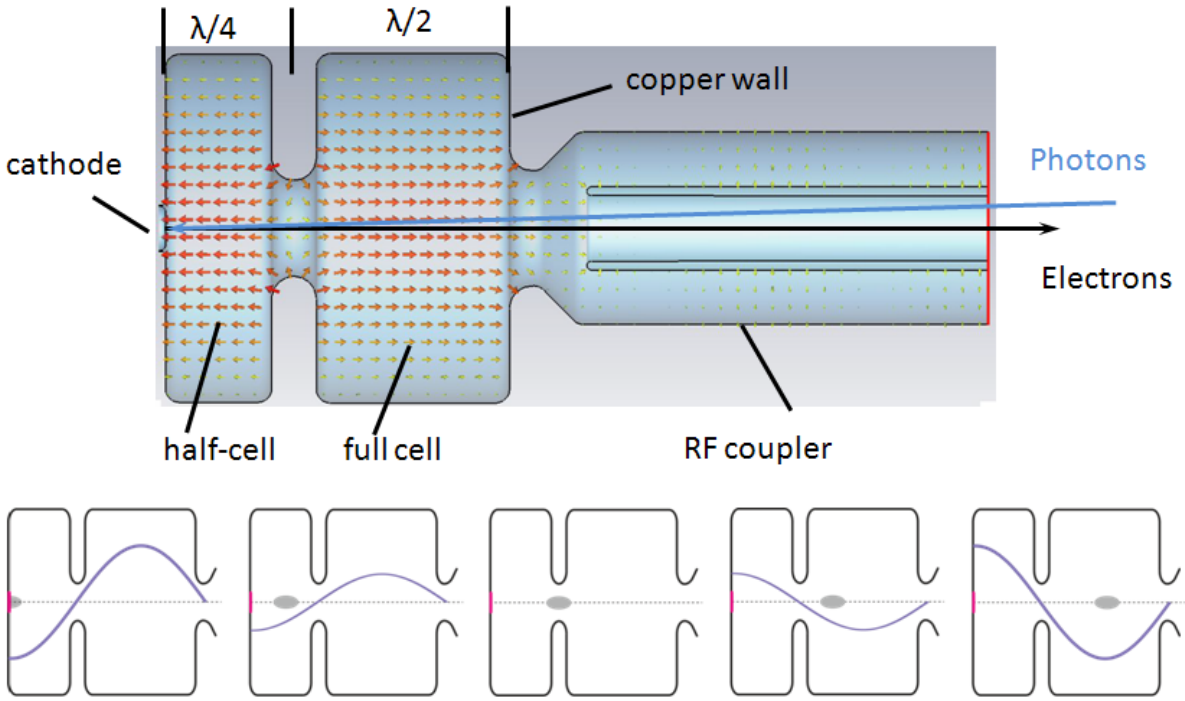

Figure 7: Schematic cross section of the AREAL RF Gun (top). The arrows indicate the strength and direction of the electric field at a certain time. The RF wave is coupled in through the coaxial RF coupler on the right. The incoming laser beam (photons) is directed through the inner conductor of the coupler toward the cathode on the left. The electrons leave the gun also through the inner conductor.

4.1 RF field description

Cylindrically symmetric electromagnetic fields can be described in the form of polynomial expansions in the radius *r*, which is especially useful for analytical calculations. For transverse magnetic RF modes (TM modes), the field is expressed to third order in *r* as

$$\begin{aligned} E_z(z,r,t,\phi) &= \left[E_{z,0} - \frac{r^2}{4}\left(E_z'' + \frac{\omega^2}{c^2}E_{z,0}\right) + \cdots\right] \times sin(\omega t + \phi), \\ E_r(z,r,t,\phi) &= \left[-\frac{r}{2}E_z' + \frac{r^3}{16}\left(E_z''' + \frac{\omega^2}{c^2}E_z'\right) - \cdots\right] \times sin(\omega t + \phi) \\ B_\theta(z,r,t,\phi) &= \left[\frac{r^2}{2}E_{z,0} - \frac{r^3}{16}\left(E_z'' + \frac{\omega^2}{c^2}E_{z,0}\right) + \cdots\right] \times \frac{\omega^2}{c^2} cos(\omega t + \phi) \end{aligned} \quad (1)$$

where E_z, E_r and B_θ are the field components in a cylindrical coordinate system (all other components are zero) and $E_{z,0}$, E_z', E_z'' and E_z''' describe the spatial on-axis dependence of the field and its first to third on-axis derivative, respectively. The angular frequency and phase of the wave are given by ω and ϕ, respectively, and c is the speed of light. It is easy to show that Eq. 1 agrees to Maxwell's equations, up to a rest, which depends on the order of the expansion.

Noting that for the fundamental spatial harmonics $E_z'' = -k^2 E_{z,0}$, $E_z'''' = -k^2 E_z'$ and $\omega/c = k$ it can be seen that all nonlinear terms in r are zero for a pure cosine like on-axis field distribution. Thus, for a pure cosine like on-axis field the exact solution is written as

$$\begin{aligned} E_z(z,t,\phi) &= E_0 \cos kz \sin(\omega t+\phi), \\ E_r(z,r,t,\phi) &= \frac{r}{2} E_0 k \sin kz \sin(\omega t+\phi) \\ B_\theta(z,r,t,\phi) &= \frac{r E_0}{2\ c} k \cos kz \cos(\omega t+\phi) \end{aligned} \qquad (2)$$

Eq. 2 is the basis for our further discussion. We will concentrate on the longitudinal dynamics thus only the longitudinal field component will be used. The transverse field components lead to focusing and defocusing forces which are relevant for the transverse dynamics, which is beyond the scope of this experiment.

4.2 Longitudinal single particle dynamics

A peculiarity of rf guns is that the electrons are generate inside a cavity. The cavity field is thus described by Eq. (2) with the cathode being located at $z = 0$. For electrons starting at $t = 0$, the longitudinal field equation yields the highest gradient at the cathode for a start phase ϕ_0 of 90°; i.e., $\phi_0 = 0°$ marks the phase where the field on the cathode changes its sign. This is the commonly used phase definition for RF guns, while for standard accelerating cavities the on-crest phase, i.e., the phase which yields the maximum energy gain, is often defined as the zero phase. The first equation of Eqs. (2) can be rewritten in the form

$$E_z(z,t) = \frac{1}{2} E_0 [\sin(\omega t - kz + \phi_0) + \sin(\omega t + kz + \phi_0)] \qquad (3)$$

The position of a particle traveling with the speed of light through the cavity is given by $z = z_0 + ct$. Since ω and k are related via $\omega/c = k$, the term $\omega t - kz$ introduces a variation of the accelerating phase at low particle velocities but becomes constant when the particles reach relativistic energies. This constant phase is called the synchronous phase. For relativistic particles, the second term in Eq. (3) describes the variation of the field amplitude inside a cell. It becomes constant (modulo 2π) when equivalent positions (i.e., separated by λ/2) are compared. (The periodicity is λ/2 because both position and time change accordingly.) By redefining the phase of the rf field as

$$\phi\,(z,t) = \omega t - kz + \phi_0 \qquad (4)$$

Eq. (3) is expressed as

$$E_z(z,\phi) = \frac{1}{2}E_0[\sin\phi + \sin(\phi + 2kz)] \tag{5}$$

A standing wave can be described as a superposition of a forward and a backward traveling wave, the two sine terms in Eq. (5) can thus be understood as these two waves. A particle traveling synchronously with the forward wave at the speed of light experiences a constant force from the forward wave but an oscillating force from the backward wave. The doubling of the oscillating frequency of the backward wave as seen by the particle is the result of the counter propagation of particle and wave. This second term does not appear in a traveling wave structure. As a basis for the following discussions, analytic approximations for the energy gain, the variation of the phase, and the bunch compression factor in the RF gun cavity will now be derived.

4.3 Energy Gain

The variation of the energy introduced by the RF field in terms of γ i.e. in terms of the ratio of the particle energy to its energy at rest, is given by

$$\frac{d\gamma}{dz} = \frac{eE_0}{2m_e c^2}[\sin\phi + \sin(\phi + 2kz)] \tag{6}$$

where e is the elementary charge and m_e is the electron rest mass. In an RF gun, the phase depends on the position, but we will follow an approach where the total energy gain is determined as a sum of contributions with a piecewise constant phase. By defining

$$\alpha = \frac{eE_0}{2m_e c^2 k}\ , \tag{7}$$

the energy gain for a constant phase in a section of length $\Delta z = z_2 - z_1$ is described as:

$$\Delta\gamma = \left\{\alpha k \Delta z \sin\phi - \frac{1}{2}\left[\cos(\phi + 2kz_2) - \cos(\phi + 2kz_1)\right]\right\}, \tag{8}$$

or for the first section

$$\gamma(z) = 1 + \alpha \left\{ kz \sin\phi + \frac{1}{2} [\cos\phi - \cos(\phi + 2kz)] \right\} \qquad (9)$$

where the integration constant has been chosen such that $\gamma = 1$ is fulfilled for all phases at $z = 0$. The second term in Eq. (8) is zero when the energy gain for a complete cell $\Delta z = \lambda/2$ is considered, and thus the energy gain is maximal at $\phi = 90°$ for full cells. In contrast, at the end of the half-cell where $kz = \pi/2$, setting $d\gamma/d\phi = 0$ in Eq. (9) yields a maximum energy gain when $\tan(\phi) = \pi/2$.

Noting that $\cos(\phi + 2kz) = \cos(2kz)\cos(\phi) - \sin(2kz)\sin(\phi)$, an approximation for small z is found as

$$\tilde{\gamma}(z) = 1 + 2kz\alpha \sin\phi \qquad (10)$$

The dimensionless parameter α represents the strength of the accelerating field. It is understood as the normalized vector potential A of a wave: $\alpha = {}^{eA}/_{mc}$ and appears in many areas of physics. Its significance comes from the fact that for $\alpha \geq 1$, the particle dynamics shows relativistic effects within one period of a wave. Describing the dynamics in terms of α allows us thus to generalize the results to a large extent. It is instructive to make a rough estimate of the energy gain in the vicinity of the cathode in the AREAL gun. The operational gradient of the gun is, thus $\alpha = 2$. With a typical starting phase of $\sin(\phi) = 0.5$, we find that the electrons already reach 90% of the velocity of light after a distance of about 0.2λ, i.e., within the half-cell of the cavity. Therefore, the phase slippage essentially takes place in the half-cell in close vicinity to the cathode. This justifies using the same phase i.e. the synchronous phase, for all cells but the half-cell. In order to take the phase slippage in the half-cell into account, the acceleration will be described in the following by a constant effective phase $\phi_{eff} = \phi_0 + \Delta\phi$ with ϕ_0 being the start phase and $\Delta\phi$ being a yet to be determined phase shift.

4.4 Phase variation and Synchronous Phase

We use Eq. (10) in order to find an approximation for the variation of the phase ϕ. With $\omega = ck$ and $dt = \frac{1}{c\beta} dz = \frac{\gamma}{c\sqrt{\gamma^2-1}}$, Eq. (4) is rewritten as

$$\phi(z) = k \int_0^z \left(\frac{\gamma}{\sqrt{\gamma^2-1}} - 1 \right) dz + \phi_0 \,, \qquad (11)$$

which can be integrated after substituting Eq. (10) for γ (with $\phi = \phi_{eff}$) to yield

$$\phi(\tilde{\gamma}) = \frac{1}{2\alpha \sin \phi_{eff}} \left[\sqrt{\tilde{\gamma}^2 - 1} - (\tilde{\gamma} - 1) \right] + \phi_0 \qquad (12)$$

The asymptotic value of the phase for $\tilde{\gamma} \gg 1$, i.e., the synchronous phase, is found from
Eq. (12) to be

$$\phi_{sync} = \frac{1}{2\alpha \sin \phi_{eff}} + \phi_0 \qquad (13)$$

4.5 Bunch Compression

The synchronous phase depends on the start phase in a nonlinear manner. If we observe two particles, representing the head and the tail of an electron bunch and therefore starting at slightly different phases ϕ_0 and $\phi_0 + \Delta\phi_0$, we will find the phase difference changing as the particles travel through the cavity. The difference of the synchronous phases of these two particles divided by the difference of the start phases describes the ratio of the final temporal distance to the initial temporal difference, a quantity referred to as the bunch compression factor. It is calculated by the derivative of the synchronous phase with respect to the start phase as

$$\frac{\Delta\phi_{sync}}{\Delta\phi_0} = 1 - \frac{\cos \phi_{eff}}{2\alpha \sin^2 \phi_{eff}} \qquad (14)$$

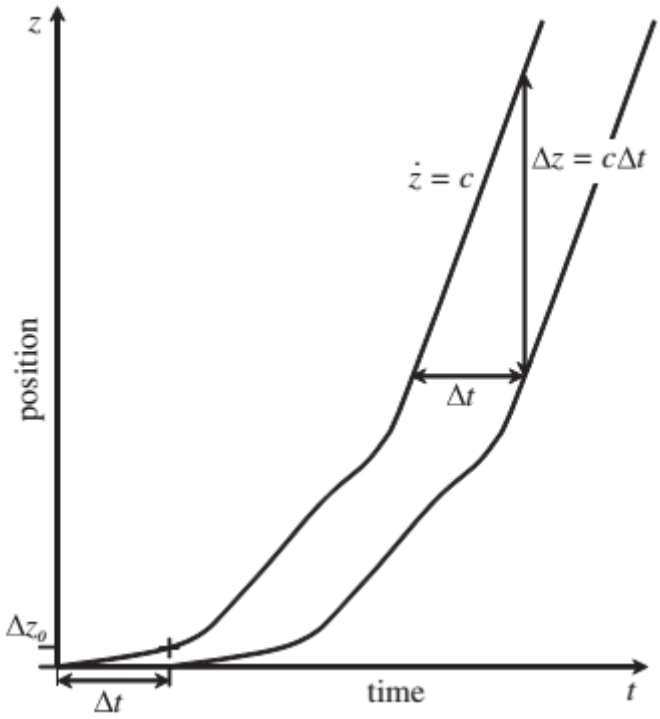

Figure 8: Schematic illustration of the acceleration of two electrons in a static field. The spatial distance of the electrons expands during the acceleration and approaches the value $\Delta z = c\Delta t$.

Figure 8 illustrates the acceleration process of two electrons in an arbitrary field by plotting position versus time $z - t$. The electrons start at the same position but with a temporal difference Δt. Figure 8 shows the case of a static field; i.e., the second (tail) electron is accelerated in the same way as the first (head) electron and its trajectory in the $z - t$ diagram is only a parallel shifted copy of the trajectory of the head electron. At any time, the spatial bunch length is given by the difference of the positions of the two electrons. The distance is very small at the time of emission of the second electron, in non-relativistic approximation $\Delta z_0 = \frac{e}{2m} E(\phi_0)\Delta t^2$, where $E(\phi_0)$ represents the longitudinal gradient at the emission phase. However, since the particles reach relativistic energies, the derivative of the trajectories in the $z - t$ diagram approaches the speed of light and the bunch length becomes $\Delta z = c\Delta t$. Any difference in the acceleration process of the two particles will lead to a variation of the final bunch length. With a stronger acceleration of the tail electron (higher phase), it will reach the speed of light earlier, and hence the bunch length will become shorter, while a reduced acceleration will lead to a longer bunch. While the temporal extension of the bunch is increased or decreased due to the phase difference of the

acceleration process, the bunch starts spatially in any case much shorter than the final bunch length, and the differences in the acceleration lead only to a suppression or promotion of the “natural” bunch expansion.

We still have to find a relation to determine the effective phase ϕ_{eff}. In order to do so, we consider the bunch compression process for different start phases in an RF gun for a short bunch. Short means that the bunch extends only over a few degrees in the RF phase. When the start phase is close to zero, the phase slips considerably when the electrons are still at low energy, i.e., in the half-cell of the cavity. The synchronous phase will, however, stay below 90°. A particle starting in the tail of the bunch will hence travel from the cathode up to the end of the cavity on a higher phase than a particle in the head of the bunch; i.e., it will be more rapidly accelerated, leading to a significant bunch compression. If the start phase, on the other hand, gets closer to 90°, the synchronous phase will become larger than 90°, the tail particle will receive a smaller acceleration, and the bunch will be decompressed. In between must be a phase where the bunch compression factor is equal to one. This phase is close to the case where the synchronous phase is 90° as will be shown below. From Eq. (14), the condition of a unit bunch compression factor is given as

$$\frac{\Delta\phi_{sync}}{\Delta\phi_0} := 1, \qquad -\frac{\cos\phi_{eff}}{2\alpha\sin^2\phi_{eff}} = 0 \tag{15}$$

which is achieved with $\phi_{eff} = \pi/2$. Setting $\phi_{eff} = \phi_{sync} = \pi/2$ into Eq. (13) yields the start phase for which the synchronous phase will become $\pi/2$:

$$\phi_0 = \frac{\pi}{2} - \frac{1}{2\alpha} \tag{16}$$

The definition of the effective phase $\phi_{eff} = \phi_0 + \Delta\phi$ leads to the generalized conclusion

$$\phi_{eff} = \phi_0 + \frac{1}{2\alpha} \tag{17}$$

5 Space charge field of a bunched beam

In the discussion above space charge has been ignored while it is very significant in practice. We already presented the space charge limits during the particle emission which restricts the maximum charge we can extract into one bunch for a given accelerating field and a given radius of the emission spot. Note that we want to reduce the radius of emission as much as possible, because the quality of the electron bunch gets higher, i.e. the transverse emittance gets smaller, when the emission area is reduced. Thus parameters are chosen such that the emission approaches the space charge limit toward the end of the emission.

Space charge repulsion leads to an increased bunch length and also in the transverse direction the bunch is defocused. Moreover it can lead to a significant grows of the beam emittance. Note however, that neither the average phase of a bunch, nor the development of the phase during the acceleration process, are influenced by space charge. Thus also the energy of the bunch is not influenced. (For long bunches a small reduction of the average energy is seen because particles are travelling on different phases.)

Space charge continues to push particles apart also when the electron bunch is further accelerated; however, the strength of the space charge force reduces with increasing energy. This is seen by an electrostatic calculation of the electric space charge field in the rest frame of the electron bunch. According to the Lorentz transformation the longitudinal coordinate is increased by a factor γ in the rest system of a bunch which moves with a velocity $c\beta = c\sqrt{1 - {}^{1}/_{\gamma^2}}$ in the laboratory system. If we assume for simplicity a simple cylindrical particle cloud the longitudinal on-axis force can be calculated by direct integration. The result depends in general on the ratio of the bunch radius to the bunch length and on the position within the bunch. Here we present only the limit for long bunches (bunch length *L* >> bunch radius *R*) at the position $z = z_{rms}$:

$$F_z = \frac{\sqrt{3}eQ}{2\pi\varepsilon_0 L^2}$$

with the total charge in the bunch *Q*.

Since *L* is the bunch length in the rest system of the bunch, and thus $L = \gamma L_{Lab}$, the force shrinks as ${}^{1}/_{\gamma^2}$.

Note that the longitudinal force does not change we transform back into laboratory system. The transverse electric field in the rest system is also proportional to $^1/_L$ and reduces thus with increasing energy:

$$\bar{E}_r = \frac{Qr}{2\pi\varepsilon_0 R^2 L} = \frac{Qr}{2\pi\varepsilon_0 R^2 \gamma L_{Lab}}$$

Here $\bar{E}_r$ is the radial electric field in the rest system

However the back transformation of the transverse field is more complex. When transforming back into the laboratory system the radial electric field of the rest system needs to be multiplied by γ. Thus the $^1/_L$ scaling in the rest system and the multiplication with γ compensate each other and we find that the transverse electric field is independent of the beam energy. Moreover a corresponding azimuthal magnetic field $B_\theta = \beta\gamma\, ^{\bar{E}_r}/_c$ is generated in the laboratory system. The transverse force in the laboratory system scales thus as:

$$F_r = e(E_r - c\beta B_\theta) = e\gamma\bar{E}_r(1-\beta^2) = \frac{eQr}{2\pi\varepsilon_0 R^2 L_{Lab}}\left(1 - \frac{\gamma^2-1}{\gamma^2}\right) = \frac{eQr}{2\pi\varepsilon_0 \gamma^2 R^2 L_{Lab}}$$

Thus while the electric field is independent on the beam energy the transverse force scales with $^1/_{\gamma^2}$ just as in the longitudinal case. A rapid acceleration to high energies as it happens in an RF gun helps thus to reduce the detrimental effects of the space charge field.

6 Outline of the Experiments

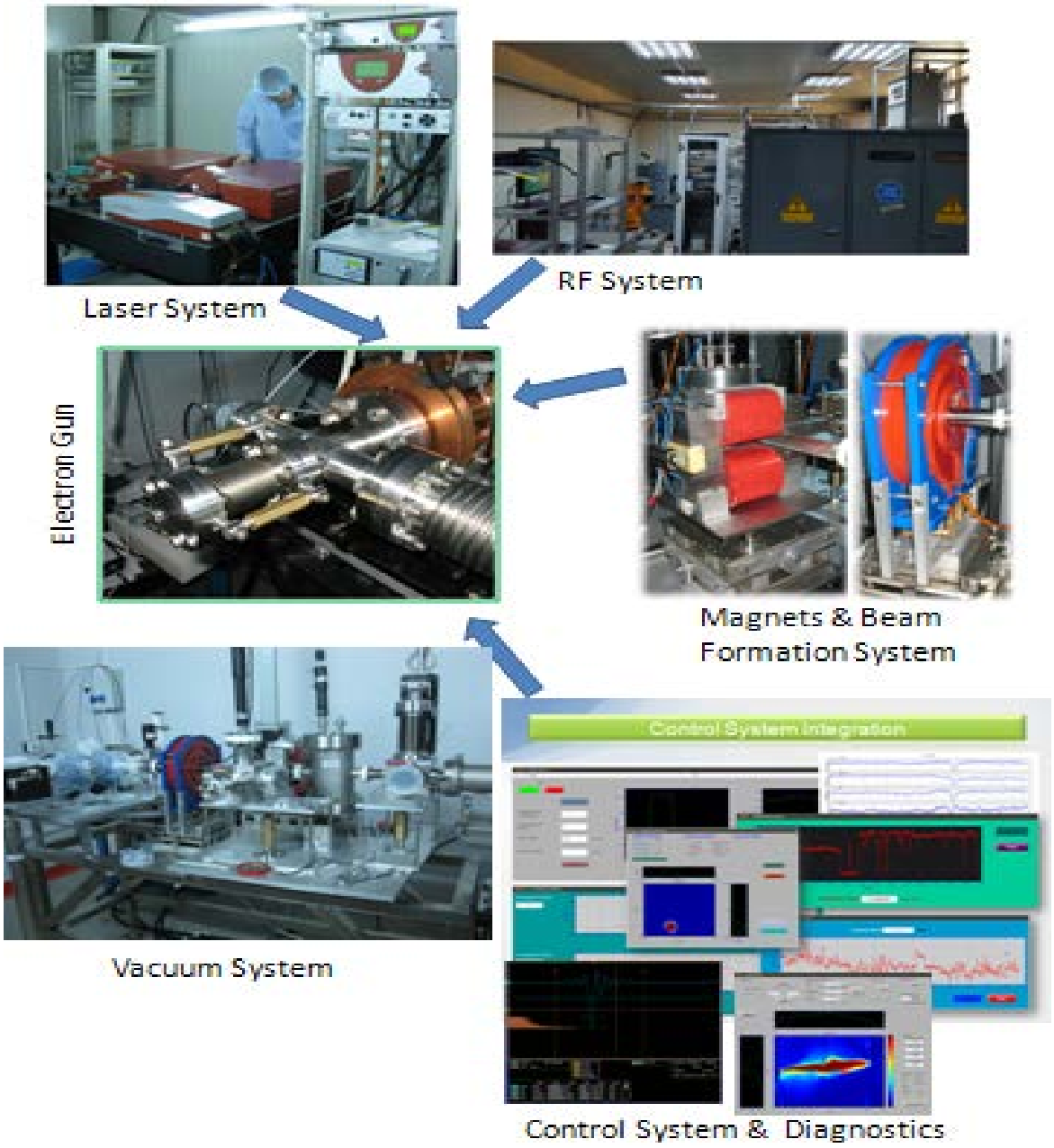

Figure 9: AREAL gun and subsystems required for the operation. In order to adjust the resonant frequency of the cavity its temperature needs to be regulated to high precision with the cooling system. The accelerating field in the gun is build up by an electromagnetic wave which is generated by the klystron transported through waveguides and coupled into the gun through the RF coupler. The gun cavity and the waveguides can operate only under ultra-high vacuum conditions thus vacuum pumps and valves are installed. In order to control the photoemission process a laser system which is connected through a transport line with the gun is integrated. Finally a control system is required in order to adjust parameters remotely and perform measurements.

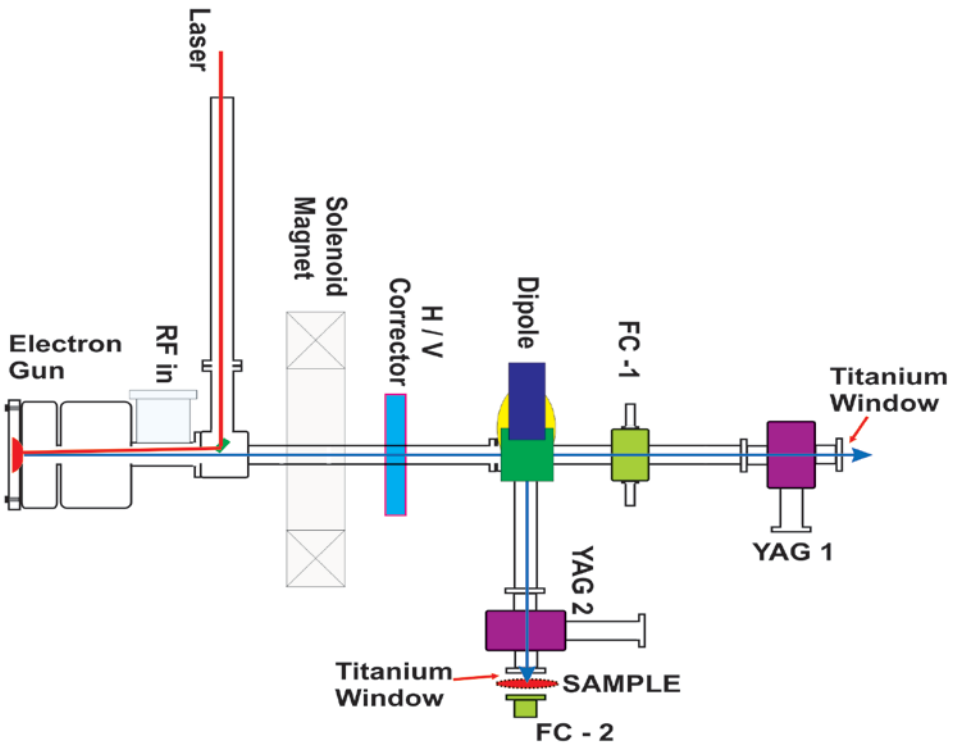

Figure 10. Schematic layout of the AREAL beamline with magnets and diagnostic components.

Figure 9 displays the AREAL gun and the subsystems required for the operation of the gun. The experiments in this course concentrate on the emission and the beam formation in the gun. The RF gun is however a complex system which requires numerous subsystems for its operation. Some subsystems are worked on in other experiments, e.g. RF properties in [9], vacuum technology in [10] and laser technology in [11]

The photoemission in the AREAL gun is triggered by a laser pulse which is directed through the laser transport path, a hole in the tunnel ceiling and an in-vacuum mirror onto the photo cathode, see Figure 10. Downstream of the gun several elements for the control and the diagnostics of the electron pulses are installed. The beam can be focused with the solenoid or transversely steered by the corrector magnets (horizontal and vertical). The beam charge can be measured in the straight beam path by means of a Faraday cup, or the beam can be bend by the 90-degree dipole magnet and observed on a screen. The screen is made of the scintillating material YAG and a camera for the observation.

6.1 Experimental Work 1

In the first experiment the quantum efficiency of the copper photo cathode installed in the AREAL gun shall be determined. This requires to measure the extracted charge on the straight line Faraday Cup. The charge collected by the Faraday Cup is flowing over a resistance to ground. The resistor is the internal resistor of an oscilloscope, so that the voltage over the resistor can be measured and displayed. The voltage follows Ohms law, i.e. it can be converted into a current flowing through the resistor. The integral over the current pulse is the total charge collected by the Faraday Cup.

In order to measure the quantum efficiency it is necessary that all electrons extracted from the cathode reach the Faraday Cup. This is achieved adjusting the focusing solenoid and the corrector magnets so that the measured charge is maximal. Moreover the gun should be operated such that the emission is not limited by the space charge field. This requires to maximize the extraction field (RF power, resonance frequency) and the start phase so that the charge reading is maximal. Reducing the pulse energy of the incident laser reduces the emitted charge and thus reduces also the space charge field. This has to be balanced with the sensitivity of the charge measurement. If the emission is not space charge limited the extracted charge depends linearly on the incident pulse energy of the laser.

From the measured charge and the measured pulse energy of the laser the quantum efficiency can be calculated as discussed in section 2.3.

The following basic parameters are required:

- Planck's constant $h = 6.62607 \times 10^{-34}$ [J· s]
- Speed of Light $c = 2.99792 \times 10^{8}$ [m/s]
- Laser central wavelength $\lambda = 258 \times 10^{-9}$ [m]
- Electron Charge $q_e = 1.60218 \times 10^{-19}$ [C]
- UV laser pulse energy $E_{UV} = 350 \times 10^{-6}$ [J] (to vary, to measure)
- Electron beam charge Q = [C] (to be measured)

Table 3 summarizes measured values of the quantum efficiency for various photo cathodes for comparison

Table 3 Typical measured values of QE for several photocathode materials

Cathode material	**λ(nm)**	**QE (%)**	**Type**	**drive laser at given λ**
Cs3Sb	527	4	semiconductor	2nd harmonic Nd:YLF
Cs2Te	263	13	semiconductor	4th harmonic Nd:YLF
K2CsSb	527	8	semiconductor	2nd harmonic Nd:YLF
Na2KSb	532	4	semiconductor	2nd harmonic Nd:YAG
Na2KSb(Cs)	532	10	semiconductor	2nd harmonic Nd:YAG
Mg	266	6×10^{-4}	Metal	4th harmonic Nd:YAG
Cu	266	1.4×10^{-4}	Metal	4th harmonic Nd:YAG
Ba	337	0.08	alkaline earth	N2
(Cs)W	375	0.11	coated metal	at UMD teststand, GaN diode
(Cs)GaAs	532	5	NEA	2nd harmonic Nd:YAG

6.2 Experimental Work 2

In the second experiment the energy of the electron pulse shall be measure as function of the RF phase. The result should be compared with the analytical relations derived in section 4.

The total energy of the electron beam at the exit of the gun is calculated by adding the energy gain in the half cell and the energy gain in the full cell. For the energy gain in the half cell take Eq. 10 and the effective starting phase given by Eq. 17. For the full cell take Eq. 8 and introduce the synchronous phase given by Eq. 13. Note that the analytical calculation yields the total energy, while you determine only the kinetic energy in the measurement. Thus for the comparison the rest mass needs to be added or subtracted.

For the measurement the beam is directed by means of the dipole magnet onto the YAG screen, see Figure 10. For each phase setting the dipole current is chosen such that the beam is in the center of the screen. The adjustment is facilitated by changing the solenoid current in order to focus the beam onto the screen. Figure 11 shows the relation of electron beam energy and measured current of the dipole.

$$E[MeV] = 299.9 * \frac{10^{-5} L_{eff}[cm]}{\Delta\alpha[rad]} * \chi * B_0[mT] \xrightarrow{\Delta\alpha=\pi/2} 0.02919 * B_0[mT]$$

According to measurements of the dipole field for the applied current, in the range from *0* to *5 A,* the relation of the B_0 dipole field to the applied current is linear and could be written as

$$B_0[T] = 0.02948 \times A\ [Amperes]$$

Note, that the RF phase at AREAL has an arbitrary offset as compared to the definition used in the theory section. Comparing the measured energy with the analytical relations allows to determine the amplitude of the accelerating field in the gun and the offset of the RF phase.

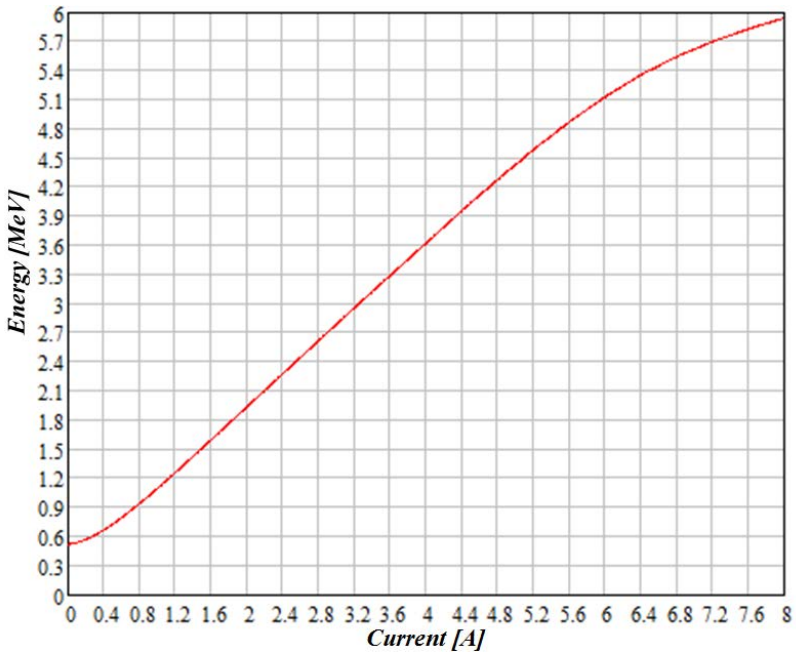

Figure 11. AREAL dipole magnet. Electron Beam Energy vs Dipole current.

6.3 Experimental Work 3 .

In the third experiment the extracted charge as function of the RF phase shall be measured. This ‘phase scan’ is a standard measurement as it allows to gain a lot of information. The interpretation of the measurement is however not always easy.

The charge is measured again by means of the straight line Faraday Cup. For each setting the solenoid and the steerers may be adjusted. The measurement can be performed for various acceleration voltages (Klystron HV 80, 110, 125 and 140 kV) and/or various laser intensities. In this way the influence of space charge effects and of the Schottky effect are altered. In order to understand the phase setting the measurement should be compared to the measurement of the energy vs phase from Experiment 2

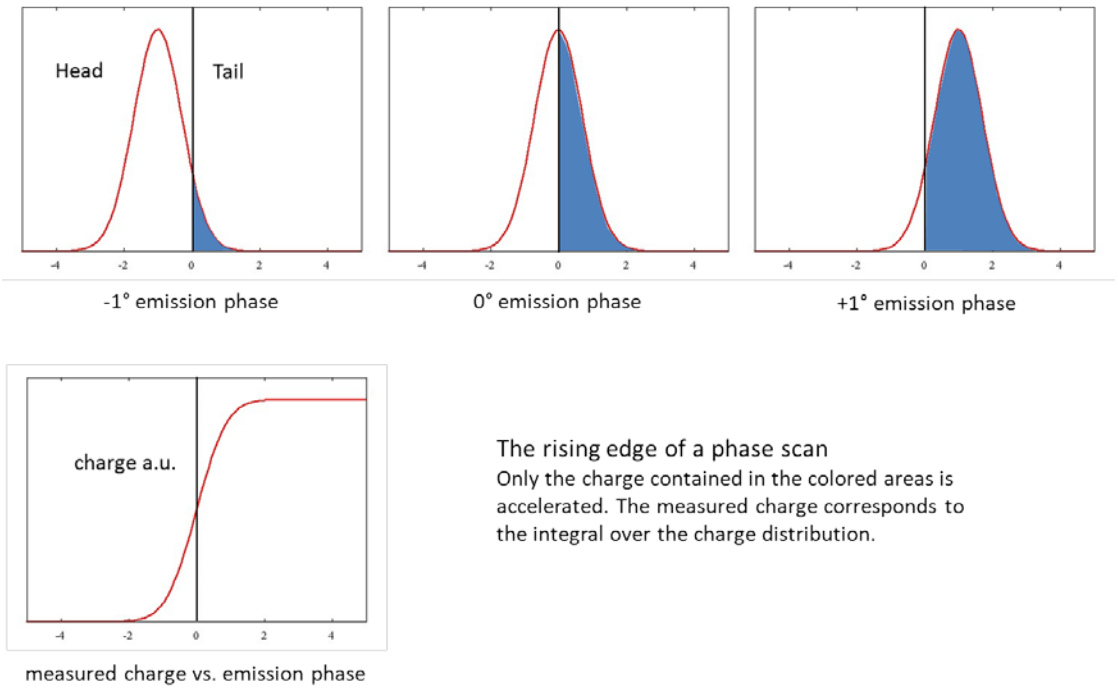

Figure 12. Sketch of the formation of the rising edge without space charge. At the zero phase (defined by the change of the sign of the accelerating field) half of the charge is extracted. The derivative of the rising edge allows to estimate the length of the incoming laser pulse. In practical applications this is limited by the space charge field. (Try to reduce the laser energy as much as possible.)

Figure 12 explains schematically the formation of the rising edge of the phase scan and its relation to the theoretical zero phase.

The falling edge of the phase scan is determined by the phase shift occurring in the gun. When the start phase is too large electrons reach the full cell on a decelerating phase. This leads to the reduction of the beam energy at higher start phases. When the phase is further increased electrons are stopped in the full cell and finally are accelerated back to the cathode.

Figure 13 discusses the phase scan in terms of space charge and Schottky effect.

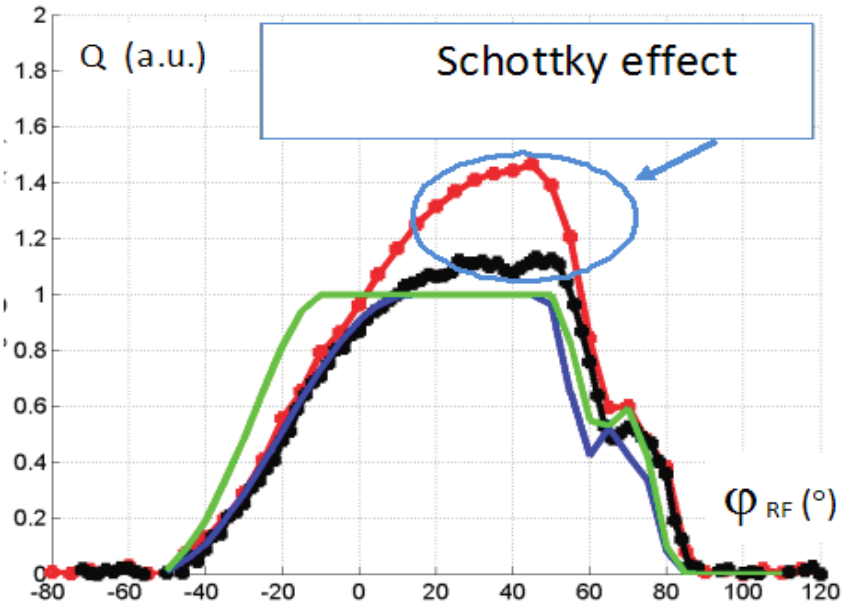

Figure 13.. Schematic of measured charge vs phase for different gun settings. The RF phase has an arbitrary offset as compared to the theoretical description. Space charge effects are significant especially at the rising edge of the scan. Here the emission phase is low and thus the extracting field is also low. The green curve shows an idealized emission as it would occur without space charge. The space charge field leads to less steep rising edge as compared to a case without space charge (black and red curve). When the extraction field (amplitude and phase) is high additional charge can be emitted due to the Schottky effect (red curve).

10 References

1. This course “Beam diagnostics and instrumentation in linear accelerators”
2. J. W. Wang and G. A. Loew, Field Emission and RF Break-down in High-Gradient Room-Temperature Linac Structures, SLAC PUB 7684, 1997.
3. H. Delsim-Hashemi, K. Floettmann, “Dark Current Studies at Relativistic Electron Gun for Atomic Exploration – REGAE”, Proceedings of IPAC2014, pp. 649-651.
4. Dekker, Adrianus J. “Schottky Effect.” AccessScience, McGraw-Hill Education, 2014.
5. K. Floettmann “RF-induced Beam Dynamics in RF Guns and Accelerating Cavities” PRST-AB 18, 064801 (2015).
6. V. M. Tsakanov, R. M. Aroutiounian, G. A. Amatuni, et al., “AREAL Low Energy Electron Beam Applications in Life and Materials Sciences“, Nuclear Instruments and Methods in Physics Research A, v.829, pp. 248-253, 2016.
7. Albert Einstein, “Zur Elektrodynamik Bewegter Körper,” Annalen der Physik 17, 891-921 (1905).
8. J.D. Jackson, Classical Electrodynamics, 3rd ed., John Wiley&Sons, 1998, 833p.
9. H. Wiedemann, Particle Accelerator Physics, v.1, Springer, 1999, 449 p.
10. This course “Radiofrequency techniques in accelerators”
11. This course “Vacuum technology in accelerators”
12. This course “Femtosecond lasers for linear electron accelerators”